THE EFFECTS OF CONCENTRATION ON THE OPTICAL PROPERTIES OF MANGANESE ALLOYED COPPER (II) SULPHIDE THIN FILMS DEPOSITED BY CHEMICAL BATH DEPOSITION TECHNIQUE.

***Akunna, J.C.C[1]., Ezenwaka, Laz[1]., Otti, I. E[1]., and Umeokwonna, N.S[1].**

1. Department of Industrial Physics, Chukwuemeka Odumegwu Ojukwu University, Uli Campus, Anambra State, Nigeria
***Corresponding author: ajimaji92@yahoo.com**

ABSTRACT
The effect of concentration on the optical properties of manganese alloyed copper (II) sulphide thin films deposited on a glass substrate was studied. The CuMnS thin films were deposited using chemical bath method. The bath for the deposited CuMnS thin films was composed of copper (II) chloride dihydrate, ($CuCl_2.2H_2O$), thiourea (H_2NCSNH_2),di-sodium-ethylene-diamine-tetra-acetic acid (EDTA), tri-ethanol-amine (TEA), manganese tetra-oxo-sulphate (VI) monohydrate and ammonium hydroxide (NH_4OH) as pH adjuster. The deposition was maintained at room temperature of 300K in alkaline medium. Results of the work show that the films have low absorbance, low reflectance, high transmittance and high refractive index in UV-VIS-NIR regions. The absorbance, reflectance, refractive index and extinction coefficient increased as concentration of Mn^{2+} ion increased while transmittance decreased as it increased. The films have wide band-gap which ranged from 2.3eV to 3.3eV and is a good material for optoelectronic application.

Key words: Characterization, Concentration, Semiconductor, Band-gap, and Thin films.

1. INTRODUCTION

The material scientists and engineers ability to conceive the novel materials with extraordinary combination of chemical, physical and mechanical properties has changed the modern society. The field of low dimensional materials, such as the thin films, has played a significant role towards that direction. Materials in thin films form represent the major component of advanced electronics, photovoltaic technology, protective coatings technology and functional nano-devices [1].

Many industries throughout the world are involved in thin films because it plays a vital role in nearly all-electronic and optical devices. It has been used as electroplated films for decoration and protection [2]. They have long been used as antireflection coatings on window glass, video screens, camera lenses and other optical devices[3]. An important question regarding thin films is concerned with the structural and dynamic changes that can occur upon replacement of either cations or anions in the binary or ternary base material. Modern day technology requires several types of thin films materials, which have been attracting an increasing interest for a variety of applications [4].Thin films can be made of single or multi- compound (binary, ternary, or quaternary) depending on the elemental composition, alloy / compound or multilayered coatings on substrates of different types, shapes or sizes [5]. As with other elements, the simplest compounds of copper are binary compounds, the principal examples being oxides, sulphides, and halides. Both cuprous and

cupric compounds are known. Among the numerous copper sulphides, important examples include copper (I) sulphide and copper (II) sulphide. Copper (II) sulphides, (CuS) belong to the IB-VI compound semiconductor materials and are among the chalcogenide compounds with several applications in nano-sciences. They are found very useful in coating solar energy conversion systems and solar controlled devices. The chalcogenides are also used in the fabrication of microelectronic devices, optical filters as well as in low temperature gas sensor applications [6]. Moreover, ternary copper chalcogenides, like copper sulphide, in recent times, are now widely used in the fabrication of solar photovoltaic cells [7]. Special attention is given to the study of copper sulphide thin films due to the discovery of the CdS/Cu_xS heterojunction solar cell [6]. CuMnS have the ability to produce multicolour emission such as blue, green and even red depending upon the Cu^{2+} ions lying on the interstices in the lattice. However, less work has been done till date on metal alloying into CuS. Therefore, it is desirable to alloy CuS particles with metals like Mn, singly and to study their structural and optical properties.

It is, therefore, important to use chemical bath deposition technique which is simple, cost-effective, environment friendly to deposit the manganese alloyed copper (II) sulphide thin films for the study of the effect of concentration on the optical properties.

2. MATERIALS AND METHODS

The chemicals used in this research include the following:- di-hydrated copper (II) chloride ($CuCl_2.2H_2O$) serving as source of Cu^{2+} ion, de-ionized water, thiourea (H_2NCSNH_2) serving as source of S^{2+} ion, hydrated manganese tetra-oxo-sulphate (VI) ($MnSO_4.H_2O$), which serves as a source of Mn^{+2} ions, ethylene-diamine-tetra-acetic acid di-sodium salt (EDTA) ($C_{10}H_{14}N_2O_8Na_2.2H_2O$) serving as complexing agent, tri-ethanol-amine (TEA) ($C_6H_{15}NO_3$) also serving as complexing agent, glass slide substrates. All the chemicals mentioned above are of analytical grade. Two complexing agents were used to yield effective deposition, as only one complexing agent could not give impressing result within the stipulated time lapse.
The slides before used were degreased in tri-oxo-nitrate (V) acid for 48 hours, washed in cold water with detergent, rinsed with distilled water and dried in air. The degreased cleaned surface provide nucleation centre for growth of the films, hence yielding highly adhesive and uniformly deposited films. The experiment was carried out at an average room temperature of 300K.

In making the solutions of the chemicals, the source of the alloying metal Mn^{2+} ion ($MnSO_4.H_2O$) compound was prepared in five sets of concentrations of 0.010M, 0.020M, 0.030M, 0.040M and 0.050M for the five setups of the experiment while the concentration of other precursors were kept constant as shown in Table1. Measured volumes of the precursors were put in 100ml beaker for each of the five concentration setups (reaction baths) as shown in Table1. Cleaned substrate was immersed in each reaction bath through synthetic foam and allowed to stand for 24 hours. Characterization apparatus used in this technique include a 2.1-Janway 6405 UV – VIS model of spectrophotometer for absorbance, XRD Machine for XRD structural analysis and EDX machine (Pocket III, Model P530) for EDXS compositional analysis.

The stepwise reactions involved in the complex ion formation and film deposition processes for CuMnS are stated below. Sulphide, S^{2-}, ions are released by the hydrolysis of thiourea,(H_2NCSNH_2)., and Cu^{2+} ions are released from the complex ion formed by the reaction of copper (II) chloride,($CuCl_2$) with EDTA and TEA.

$$CuCl_2 + EDTA \rightarrow Cu[EDTA]^{2+} + 2Cl^-$$
$$Cu[EDTA]^{2+} \rightarrow \boldsymbol{Cu^{2+}} + [EDTA]^{2-}$$
$$MnSO_4 + TEA \rightarrow MnTEA^{2+} + SO_4^{2-}$$
$$Mn[TEA]^{2+} \rightarrow \boldsymbol{Mn^{2+}} + TEA^{2-}$$
$$[NH_2]_2CS + OH^- \rightarrow [NH_2]_2CO^+ + HS^-$$
$$HS^- + OH^- \rightarrow H_2O + \boldsymbol{S^{2-}}$$
$$\boldsymbol{Cu^{2+}} + \boldsymbol{Mn^{2+}} + \boldsymbol{S^{2-}} \rightarrow \boldsymbol{CuMnS}$$

Table 2.1. Variation of concentration of alloying metal for CuMnS thin film deposition at average room temperature

BATH NAME	$MnSO_4.H_2O$		$CuCl_2.2H_2O$		EDTA		TEA		Thiourea		NH_4OH Vol. (ml)	Time (Hrs)	pH	Temp. (K)
	Conc. Mol/dm^3	Vol. (ml)	Conc. Mol/dm^3	Vol. (ml)	Conc. Mol/dm^3	Vol. (ml)	Conc. Mol/dm^3	Vol. (ml)	Conc. Mol/dm^3	Vol. (ml)				
CuMnSc$_1$	**0.01**	10	0.5	5	0.5	5	0.5	5	0.25	10	10	24.0	11.0	300
CuMnSc$_2$	**0.02**	10	0.5	5	0.5	5	0.5	5	0.25	10	10	24.0	11.0	300
CuMnSc$_3$	**0.03**	10	0.5	5	0.5	5	0.5	5	0.25	10	10	24.0	11.0	300
CuMnSc$_4$	**0.04**	10	0.5	5	0.5	5	0.5	5	0.25	10	10	24.0	11.0	300
CuMnSc$_5$	**0.05**	10	0.5	5	0.5	5	0.5	5	0.25	10	10	24.0	11.0	300

3. THEORY

Calculation of optical properties

Reflectance (R) $= \boldsymbol{1 - (A + T)}$ (1)

where A is absorbance and T is transmittance [8].

Refractive index (η) $= \frac{1+\sqrt{R}}{1-\sqrt{R}}$ (2)

where R is reflectance [9]

Absorption coefficient (α) $= \frac{A}{\lambda}$ (3)

where A is absorbance, and λ is wavelength [10][11]

Extinction coefficient (K) $= \frac{\alpha\lambda}{4\pi}$ (4)

where α is absorption coefficient, and λ is wavelength [10][11].

Photon energy (eV) $= \boldsymbol{E = h\nu}$ (5)

where **h** is Planck's constant = 6.63 x 10^{-34}Js**,** and **ν** is frequency of photon.

However, $\nu = \frac{c}{\lambda}$ (6)

where **c** is velocity of light = 3.0 x 10^8m/s, and **λ** is wavelength.

Hence $E = \frac{hc}{\lambda}$, (7)

but $1eV = 1.602\,x\,10^{-19}\,J$,

Planck's constant $h = \frac{6.63\,x\,10^{-34}\,js}{1.602\,x\,10^{-19}\,j} \approx 4.14\,x\,10^{-15}\,eV$

Therefore **photon energy** $\boldsymbol{E = \frac{4.14\,x\,10^{-15}\,eV\,x\,3.0\,x\,10^{8}\,m/s}{\lambda(m)} = \cdots \ldots \ldots eV}$

This is the band-gap energy, **Eg** [12]

4. RESULTS

(i) Absorbance (A)

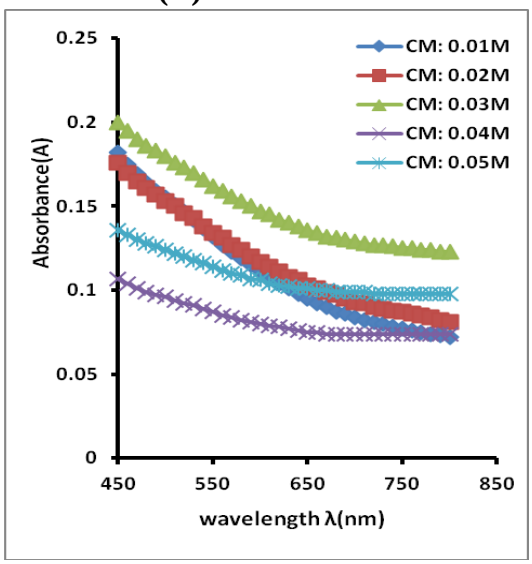

Fig. 4.1: Graph of absorbance (A) versus wavelength λ (nm) for CuMnS thin film.

(ii) Transmittance (T %)

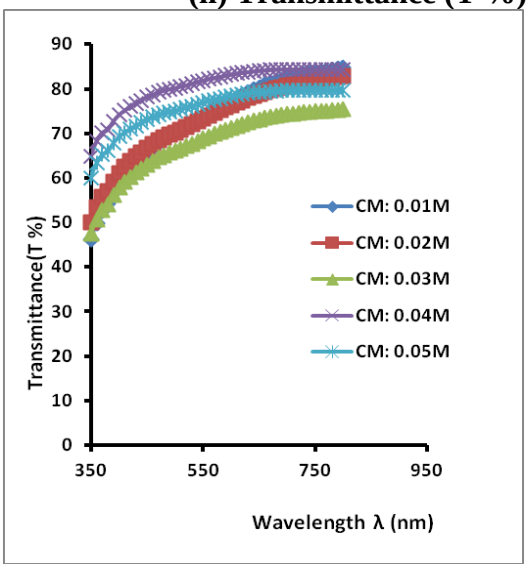

Fig.4.2: Graph of transmittance (T%) versus wavelength λ (nm) for CuMnS thin film

(iii) Reflectance (R)

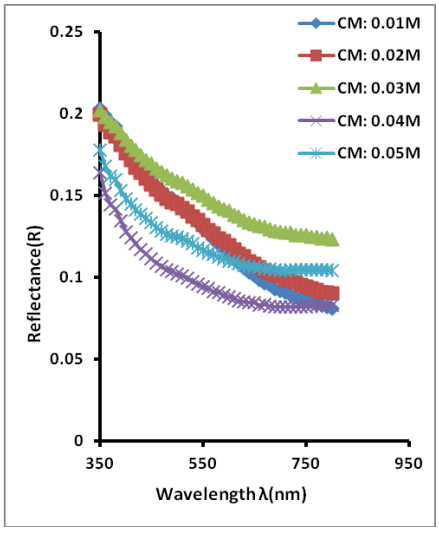

Fig 4.3: Graph of reflectance (R) versus wavelength λ (nm) for CuMnS thin film

(iv) Refractive Index (η)

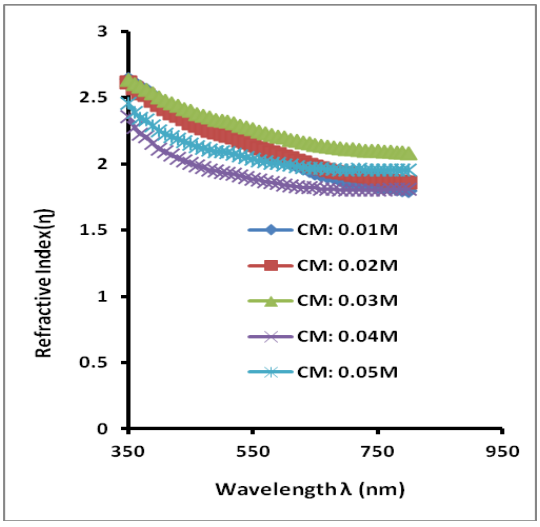

Fig 4.4: Graph of refractive index (η) versus wavelength λ (nm) for CuMnS thin film

(v) Extinction coefficient (K)

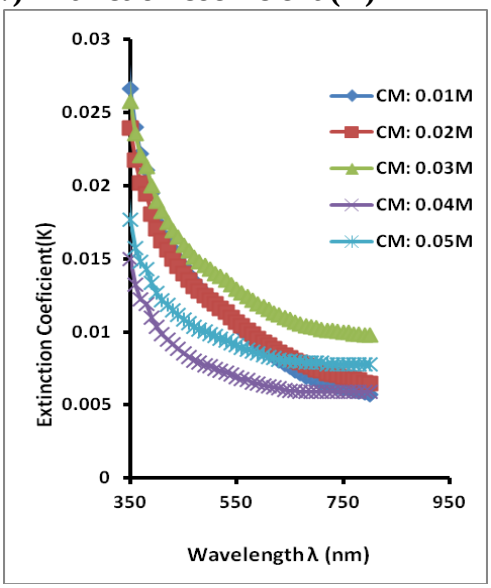

Fig 4.5: Graph of extinction coefficient (K) versus wavelength λ (nm) for CuMnS thin film

(vi) Complex dielectric constant ($\mathcal{E}_c$)

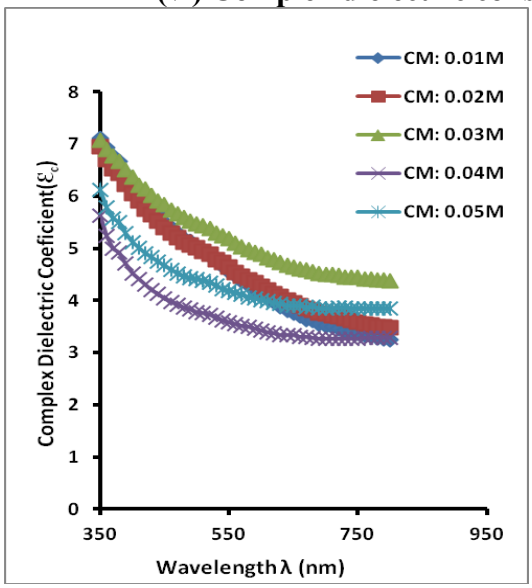

Fig 4.6: Graph of complex dielectric constant ($\mathcal{E}_c$) versus wavelength λ (nm) for CuMnS thin film

(vii) Optical thickness (µm)

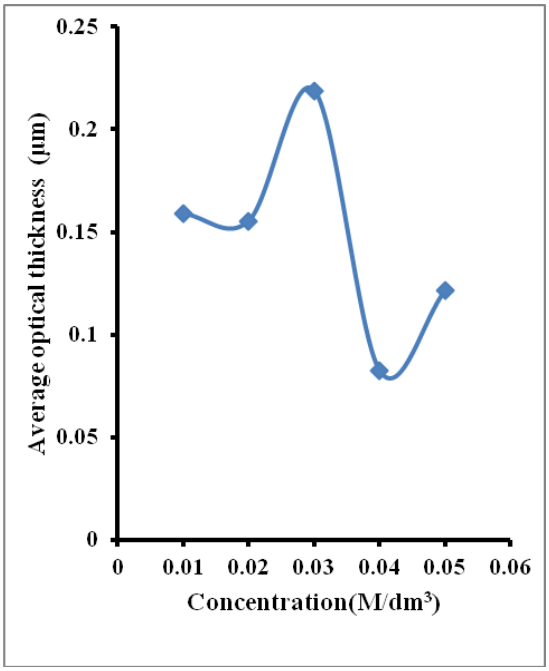

Fig 4.7: Graph of Average optical thickness (µm) versus Concentration (M/dm^3) for CuMnS thin film.

(viii) Absorption coefficient squared (α^2)

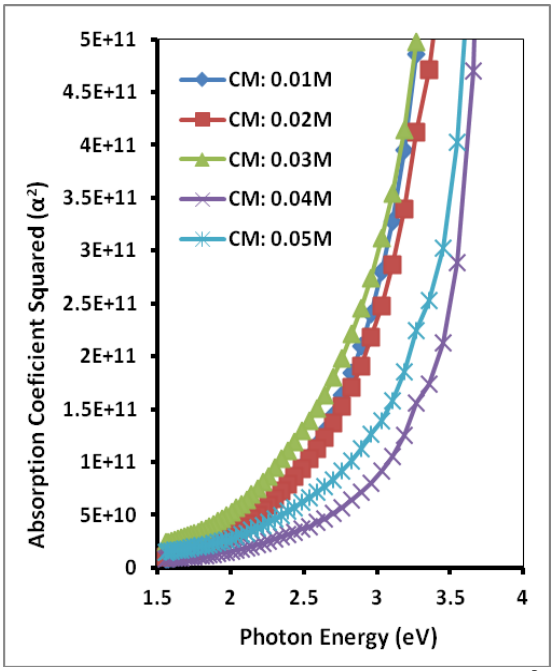

Fig 4.8: Graph of absorption coefficient squared (α^2) versus photon energy (eV) for CuMnS thin film.

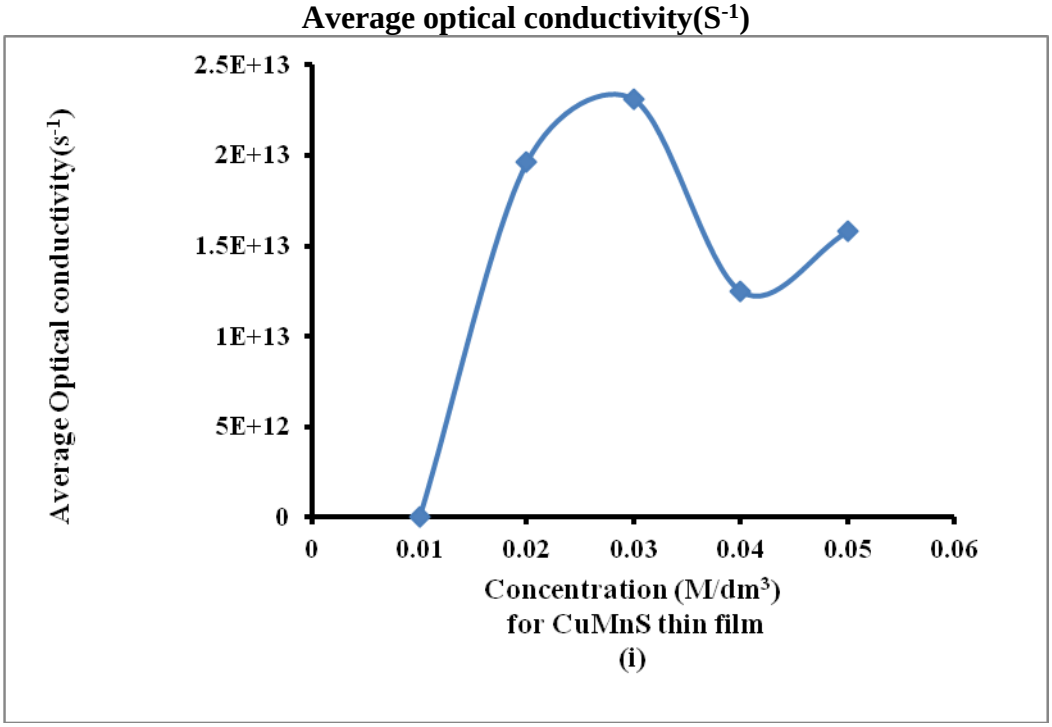

Fig.4.9: Average optical conductivity (S^{-1})

Structural properties of manganese alloyed copper (II) sulphide, (CuMnS) thin films

(a)Scanning electron microscopy (SEM) for CuMnS thin films

Fig.4.10: SEM of CuMnS thin film (0.05M concentration).

(b) Energy dispersive x-ray spectroscopy (EDXS) for CuMnS thin films

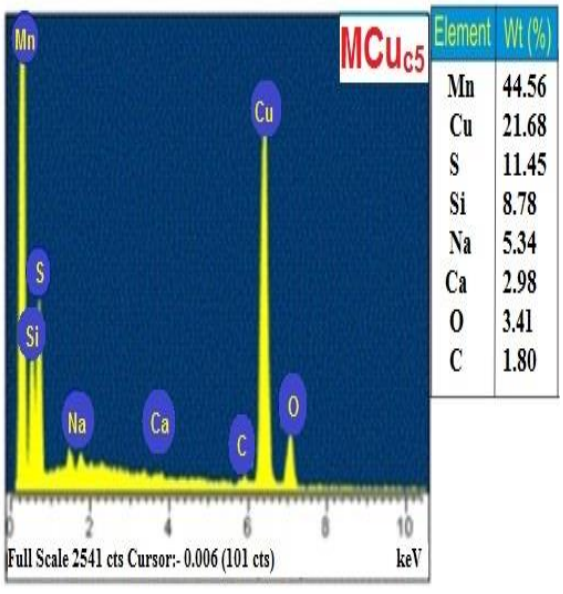

Fig.4.11: EDXS of CuMnS thin film (0.05M Concentration).

(c) X-ray diffraction (XRD) for CuMnS thin films

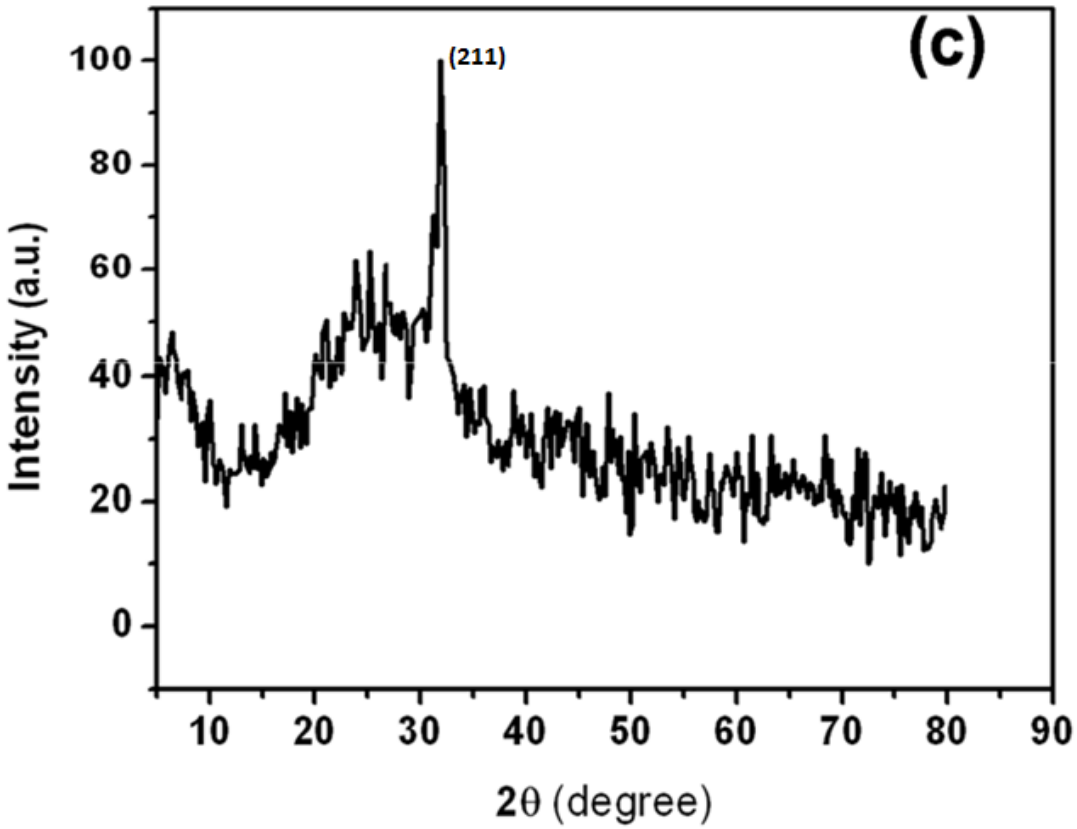

Fig.4.12: XRD pattern of CuMnS thin film.

Table 4.1 XRD Analysis of Chemically Deposited CuMnS thin film

Content	Structure	$2\theta^0$	FWHM (eV)	hkl	Lattice constants (Å)	d-spacing (Å)	Crystallite size (D) $x10^{-9}$ m	Dislocation density (ρ) $x10^{-13}$ (line m^{-2})	Microstrain (Ɛ) $x10^{-3}$
CuMnS	Hexagonal Crystalline Solid	33.30	1.50	211	a=10.585 b=10.585 c=5.383	3.532	75.20	5.655	4.599

5. Discussion

From Fig.4.1, the absorbance of the films is low, maximum of 0.20 (20%) in VIS region and decreases to minimum of 0.08 (8%) in NIR region. The absorbance decreases as wavelength increases. It increases as Mn^{2+} concentration increases. However, the thin films of the higher concentrations of 0.04M and 0.05M peeled off the substrate due to impurities which caused over thickening and the thin film started building up afresh. These chemo-dynamic reactions in the bath delayed the earlier deposition on the substrate of the thin film from the concentration of 0.04M and 0.05M. Fig.4.2 shows that the transmittance of the thin films increases as the wavelength increases. The films have high transmittance, minimum of 48.00% in UV region and maximum of 85.33% in NIR region. Transmittance of the films

decreases as Mn^{2+} concentration increases. As a result of impurities in the higher concentrations of 0.04M and 0.05M, the thin films formed peeled off the substrate and started building up afresh. Hence there is chemo-dynamic reaction in the bath which caused delay in the early deposition on the substrate. Fig.4.3 shows that the reflectance of the thin films is generally low in all the regions, maximum of 0.20 in the UV region and decreases to a minimum of 0.08 in the NIR region. The reflectance decreases as wavelength increases and increases as Mn^{2+} concentration increases. The impurities in the higher concentrations of 0.04M and 0.05M, the thin films formed peeled off the substrate and started building up afresh. High transmittance, low absorbance and low reflectance make the films good material for solar cells and photo-thermal heating. From Fig.4.4 the films have high refractive index, maximum of 2.70 in the UV region and decreases to a minimum of 1.85 in the NIR region. The refractive index decreases as wavelength increases and increases as Mn^{2+} concentration increases. Thin films of higher concentration values of 0.04M and 0.05M over thickened due to impurities and peeled off the substrate and started building up afresh. High refractive index makes the film a good material for film stack for anti-reflection coatings. From Fig.4.5 the extinction coefficient of the films decreases as wavelength increases. It is generally low, maximum of 0.027 in the UV region and minimum of 0.007 in the NIR region. It increases as Mn^{2+} concentration increases. Fig.4.6 shows that the complex dielectric constant decreases as the wavelength increases. It increases as the concentration increases. It ranges from 7.0 in the UV region to 3.5 in the NIR region. As shown in Fig.4.7, the optical thickness of the thin film ranges from 0.075μm to 0.235μm. The concentrations from 0.01M to 0.03M favoured the thin film deposition. Due to imbalance in the chemo-dynamic reactions in the bath as a result of impurities in the higher concentrations of 0.04M and 0.05M, the thin films formed peeled off the substrate and started building up afresh. From Fig.4.8, the thin films have large band-gap which ranged from 2.65eV to 3.35eV. The band-gap energy decreases as the concentration increases. This makes a material for optoelectronic materials that can operate faster and at high temperatures and voltages.

From the Fig.4.9, the optical conductivity increases as the concentration of the bath solution increases except at the concentrations of 0.04M and 0.05M. That is to say that, higher concentrations do not favour the optical conductivity.

Fig.4.10 shows the polycrystallite wavelength diffraction (WD) of 10.30mm, magnification (Mag) of 6000x, heating voltage (Hv) of 15KV, high frequency wavelength (HFW) of 124μm, pressure of 70pa (paschals), and scale measure of 15μm. The scanning electron microscopy (SEM) results of these films are conglomerate of particles of different sizes, hence polycrystalline.

From Fig.4.11, the film is composed of Manganese: 44.56, Copper: 21.68, and sulphur: 11.45. Other trace elements in the results are likely to be in the substrate as impurities. These impurities were the cause of the trend deviation in the film deposition. However the proportionality and percentage of existence in the bath solutions are not the same.

Fig.4.12 shows the XRD pattern which illustrates the multiple diffraction peaks of the copper structure. The pattern for the film displayed diffraction peaks at different 2θ values. The presence of identifiable peaks in the diffractograms suggests that the films are not amorphous but crystalline in nature. A close observation of the figure shows an improvement in the

crystallinity of the films as dip time increases. The peaks confirm the crystallinity of the films.

According to the result, in Table 4.1, the deposited thin film is crystalline which has a hexagonal structure.

The lattice constants are a = 10.585 Å, b = 10.585 Å and c = 5.383 Å. The crystallite size of the film is

75.20nm, dislocation density of 5.655 x 10^{-13} (line m^{-2}) and the microstrain of 4.599 x 10^{-3} at hkl of 211,

FWHM of 1.50eV.

6. CONCLUSIONS

The CuMnS semiconductor alloyed thin films have been deposited by chemical bath deposition technique.

Absorbance, reflectance, refractive index and extinction coefficient of the films increase as concentration of Mn^{2+} ions increase while transmittance decreases as it increases. All the optical properties mentioned above decrease as the wavelength increases, except their transmittance which increases as the wavelength increases. Their thin film semiconductor materials of all the optical properties mentioned above are more sensitive and favourable for opto-electronic devices than the doped single or binary compounds. Hence they can be used for light emission devices (LED), and multi-junction solar cells, solar cars in solar arrays, and in fiber optic temperature sensors, near-infrared laser diodes, forward-looking-infrared (FLIR) grade, cathode ray tube screens, and x-ray tube screens that glow (luminescent) in the dark, and electroluminescent panels. They are used in thin film resistors, photo-resistors (light dependent resistors), cathodoluminescence (when excited with electron beam), conductivity increases when irradiated with light (used as a photo-resistor).

The results above show that the as–grown thin films have varied band gaps and their optical values suggest that they are ternary transition metal semi-conducting thin films.

However, chemo-dynamic reactions and thermo-dynamic reactions in the bath solutions caused by impurities resulted to certain deviations in the films which led to peeling off of the thin films from the substrate due to heavy thickening and the thin films started building up afresh.

7. REFERENCES

1. Ezenwaka, Laz, Okereke, N.A. and Odezue, O.O. (2014). Effect of pH on chemical bath deposited copper nickel selenide thin films. *Inter Disciplinary Research Journal*, **1**, (1), 1-5.

2. Heavens, O. S. (1970). Thin film physics. *Photochemical and Photoelectrochemical Conversion and Storage of Solar Energy*,London, Methuen and Co Ltd. London Publishers, 331.

3. John, M. P. and King, N. T. (1980). Analysis of thin films and interfaces, *Journal of Physics Today,* **33**(5), 34 – 39.

4. Samanta, D., Samanta, B., Chaudhuri, A. K., Ghorai, S. and Pal, U. (1996). Electrical characterization of stable air – oxidized CdSe films prepared by thermal evaporation. *Semiconductor Science Technology* **11**,(4), 548 – 553.

5. Lee, J., Song, W., Yi, J. and Yoo, Y. (2003). Characteristics of the CdZnS thin films doped by thermal diffusion of vacuum evaporated indium films. *Materials and Solar Cells*, **75** (1-2), 227 – 234.

6. Ezema, F.I. (2004). Fabrication, optical properties and application of Un–doped chemical bath deposited ZnO thin films. *Journal of Research Science*, **1**(15), 343 – 350.

6. Ezema, F.I. (2004). Optical properties of chemical bath deposited FeCdS3 thin films. *Academic Open Internet Journal*, **11** (10) 44 - 65.

7. Ilenikhena, H.M., Housecroft, C. E. and Sharpe, A. G. (2008). Inorganic chemistry (3rd ed.*). Prentice Hall.* 722. ISBN 978-0131755536.

8. Janai N., Alfred D.D., Booth D.C. and Seraphin B.O., (1979), Optical Properties and Structure of Amorphous Silicon Films Prepared by CVD, Journal of Solar Energy material, **1**, (1–2), 11– 27.

9. Snell A.A., Sabra A.I., (1972), *Theories of Light from Descartes to Newton*, Cambridge University Press. (cf. Pavlos Mihas, Use of History in Developing ideas of refraction, lenses and rainbow, p. 5, Demokritus University, Thrace, Greece.) (Jin-gang *et al., 2009 in Snell, 1972*).

10. Coutts T. J., Ward J. S., Young D. L., Dessent T. A., and Noufi R., (2001), The Search for and Potential Impact of Improved Transparent Conducting Oxides on Thin Film Solar Cells, Technical digest of the 12th international photovoltaic science and engineering conference, Jeju Korea June 11-15.

11. Mahrov, B., Boschloo G., Hyfeldt A., Siegbahn H. and Rensmo H., (2004), Photoelectron Spectroscopy Studies of Ru(dcbpyH2)2(NCS)2/CuI and Ru(dcbpyH2)2/CuSCN Interfaces for Solar Cell Applications, Journal of Physical Chemistry B, **108**(31), 11604 – 11610.

12. MeMahon B., Kurtz S., Emery K., Young M., (2002), Criteria for the Design of GaIn P/Ga As/Ge Triple Junction Cells to Optimize their Performance Outdoors, 29th IEEE PVSC New Orleans.